

Experimental Evidence of the Vacancy-Mediated Silicon Self-Diffusion in Single-Crystalline Silicon

Yasuo Shimizu, Masashi Uematsu, and Kohei M. Itoh*

Department of Applied Physics and Physico-Informatics, Keio University, 3-14-1 Hiyoshi, Kohoku-ku, Yokohama 223-8522, Japan
(Received 2 November 2006; published 2 March 2007)

We have determined silicon self-diffusivity at temperatures 735–875 °C based on the Raman shift of longitudinal optical phonon frequencies of diffusion annealed $^{28}\text{Si}/^{30}\text{Si}$ isotope superlattices. The activation enthalpy of 3.6 eV is obtained in such low temperature diffusion annealing. This value is significantly smaller than the previously reported 4.95 eV of the self-interstitial mechanism dominating the high temperature region $T \gg 855$ °C and is in good agreement with the theoretical prediction for the vacancy-mediated diffusion. We present a model, containing both the self-interstitial and the vacancy terms, that quantitatively describes the experimentally obtained self-diffusivity between 735 and 1388 °C, with the clear crossover of the two diffusion mechanisms occurring around 900 °C.

DOI: 10.1103/PhysRevLett.98.095901

PACS numbers: 66.30.Hs, 61.72.Ji, 68.65.Cd

Self-diffusion investigation using silicon (Si) is important, because Si single crystal boasts unsurpassable crystalline perfection and chemical purity, which are crucial for the exclusive probing of the self-diffusion phenomena in solids. In addition, understanding of the Si self-diffusion mechanism that plays a key role in the impurity diffusion, annealing of the implantation damage, etc., is needed for the development of process simulators for future nano Si electronics. One of the major focuses of discussion is whether the vacancy-dominated diffusion, which is predicted to be important theoretically [1–8], ever takes a visible role. Bracht *et al.* [9] established that the experimental self-diffusivity ($D_{\text{Si}}^{\text{SD}}$) between 855 and 1388 °C could be described by a single exponential as

$$D_{\text{Si}}^{\text{SD}} = (530_{-170}^{+250}) \exp\left(-\frac{(4.75 \pm 0.04) \text{ eV}}{k_B T}\right) \text{ cm}^2 \text{ s}^{-1}. \quad (1)$$

Together with other studies which established the activation enthalpy $H_I = 4.95$ eV for the self-interstitial mechanism [10], they concluded that the contribution of the vacancy mechanism is very small in diffusion at such high temperatures. Accurate determination of the self-diffusivity at low temperatures $T < 850$ °C by the standard method, e.g., secondary ion mass spectrometry (SIMS) of the depth profile of the specific Si isotopes, is difficult because the diffusion length after reasonable annealing duration in the lab (< 180 days) is still too small for the depth resolution of SIMS. The present study overcomes this challenge by detection of the very small diffusion length in isotope superlattices of Si by Raman spectroscopy. The method has been proven useful in the past for the accurate determination of the self-diffusivity in Ge [11] and characterization of Si isotope superlattices [12,13].

Si self-diffusion is expected to occur predominantly via two types of native defects: self-interstitials (I) and vacancies (V) [9,10,14–18]. Thus, the Si self-diffusivity $D_{\text{Si}}^{\text{SD}}$ is expressed by

$$D_{\text{Si}}^{\text{SD}} = f_I \frac{C_I^{\text{eq}}}{C_0} D_I + f_V \frac{C_V^{\text{eq}}}{C_0} D_V. \quad (2)$$

Here $C_{I,V}^{\text{eq}}$ and $D_{I,V}$ are the equilibrium concentrations and diffusivities of I and V , respectively. C_0 is the concentration of the Si atoms. $f_I \approx 0.73$ [19] and $f_V = 0.5$ [20] are the correlation factors for interstitial and vacancy mechanisms in the diamond structure, respectively.

The vacancy term is not well-understood because the vacancy-mediated self-diffusion has never been observed directly in its equilibrium form. The enthalpy for the vacancy-mediated diffusion H_V is given by the sum of the formation and migration enthalpies: $H_V^f + H_V^m$. Experimentally reported H_V^f are 2.8 ± 0.3 [21], 2.44 ± 0.15 [22], and 2.1 ± 0.7 eV [23], while large cell size (~ 256) calculations predict slightly larger values confined between 3.1 and 3.6 eV [4–6]. In parallel, $H_V^m = 0.18$ –0.45 [24], 1.3 [21], and 1.8 ± 0.5 eV [23] are found experimentally, while theory predicts 0.4 [6] and 0.58 eV [7]. Because $H_V^m = 0.45$ eV was obtained experimentally below room temperature [24], it has been suggested that H_V^m depends on the temperature. Thus, a theoretical model has been proposed that bridges between experimental values 1.3 (or 1.8) eV for high temperatures and 0.4 (or 0.58) eV calculated theoretically for low temperatures [8]. In the present work, we show that the experimentally obtained Si self-diffusivity can be described quantitatively by a simple double-exponential equation [Eq. (2)].

A $^{28}\text{Si}_n/^{30}\text{Si}_n$ isotope superlattice with $n = 20$ atomic layers was grown by solid-source molecular beam epitaxy [12,13]. The details of the growth have been described in Ref. [13]. In short, the starting substrate was a high resistivity ($\rho > 2000$ Ω cm), n -type Si {001}-oriented 2-inch substrate, onto which a buffer layer of ≈ 100 nm-thick $^{\text{nat}}\text{Si}$ (^{28}Si : 92.2%, ^{29}Si : 4.7%, ^{30}Si : 3.1%) was formed prior to the growth of the isotope superlattice that composed of alternating layers of isotopically pure ^{28}Si (99.92%) and

^{30}Si (99.3%). The degree of intermixing at the ^{28}Si and ^{30}Si interfaces is less than a couple of monolayers in an as-grown isotope superlattice [13]. The wafer was cut into $2 \times 2 \text{ mm}^2$ squares for diffusion annealing in a resistance furnace under a pure argon (99.99%) atmosphere. The temperature inside the furnace was monitored with a Pt/PtRh thermocouple to stabilize the furnace within $\pm 2^\circ\text{C}$. The intrinsic carrier concentration was $\sim 1 \times 10^{18} \text{ cm}^{-3}$ at the lowest diffusion annealing temperature of 735°C , which ensured that the sample remained intrinsic and the Fermi level effect did not play a role. The Raman measurements of the longitudinal optical (LO) phonon frequencies were performed using an Ar^+ 514.5 nm line. The scattering light was dispersed by a single spectrometer and detected by a charge coupled device with the spectral resolution of 0.7 cm^{-1} . All spectra were recorded in the backscattering geometry with the sample temperature $T = 8 \text{ K}$.

The depth profile of the ^{30}Si concentration $C_{^{30}\text{Si}}(x, t, T)$ in the diffusion annealed $^{28}\text{Si}/^{30}\text{Si}$ isotope superlattice is given in terms of the depth x , diffusion annealing time t , and the self-diffusivity $D_{\text{Si}}^{\text{SD}}(T)$ for a given annealing temperature:

$$C_{^{30}\text{Si}}(x, t, T) = C_{^{30}\text{Si}}^d + \frac{C_{^{30}\text{Si}}^e - C_{^{30}\text{Si}}^d}{2} \times \sum_{k=1}^p \left[\text{erf}\left(\frac{x - \{(k-1)d_e + kd_d\}}{2(l + \sqrt{D_{\text{Si}}^{\text{SD}}(T)t})}\right) - \text{erf}\left(\frac{x - (kd_e + kd_d)}{2(l + \sqrt{D_{\text{Si}}^{\text{SD}}(T)t})}\right) \right]. \quad (3)$$

Here $C_{^{30}\text{Si}}^e$ and $C_{^{30}\text{Si}}^d$ are the concentrations of ^{30}Si in the isotopically enriched and depleted layers, respectively, in the $^{28}\text{Si}/^{30}\text{Si}$ isotope superlattice prior to the diffusion annealing assuming perfectly abrupt interfaces. Likewise, d_e and d_d are thicknesses of the isotopically enriched “ ^{30}Si layer” and the depleted “ ^{28}Si layer,” respectively. The degree of intermixing before diffusion annealing is introduced by the intermixing parameter l . p is the number of periods of the $^{28}\text{Si}/^{30}\text{Si}$ layers. The isotope superlattice employed in the present study has $C_{^{30}\text{Si}}^e = 0.993$, $C_{^{30}\text{Si}}^d = 0.0008$, $d_e = d_d = 2.7 \text{ nm}$, and $l \approx 2$.

The corresponding average mass of an atomic layer $M(x, t, T)$ situating at a depth x before and after annealing in the Si isotope superlattice is given by

$$M(x, t, T) = C'_{^{28}\text{Si}}(x, t, T)M_{^{28}\text{Si}} + C'_{^{30}\text{Si}}(x, t, T)M_{^{30}\text{Si}}, \quad (4)$$

where $M_{^{28}\text{Si}}$ and $M_{^{30}\text{Si}}$ are the masses of ^{28}Si and ^{30}Si atoms, respectively. $C'_{^{28}\text{Si}}(x, t, T)$ and $C'_{^{30}\text{Si}}(x, t, T)$ are the normalized concentration [i.e., $C'_{^{28}\text{Si}}(x, t, T) + C'_{^{30}\text{Si}}(x, t, T) = 1$] as introduced in Ref. [11]. Because $M(x, t, T)$ oscillates also with the periodicity $d_e + d_d$, new phonon modes whose vibrations are confined in ^{28}Si

and ^{30}Si layers emerge. The frequencies (wave numbers) of such confined phonons are very sensitive to the periodicity, d_e and d_d , and the abruptness of the $^{28}\text{Si}/^{30}\text{Si}$ interfaces given by l and $\sqrt{D_{\text{Si}}^{\text{SD}}(T)t}$. Since the interface prior to diffusion annealing is very sharp (l is only 2), the frequencies of confined phonon modes in the diffusion annealed samples are given solely by $\sqrt{D_{\text{Si}}^{\text{SD}}(T)t}$, since $d_e = d_d = 2.7 \text{ nm}$ remain unchanged for any annealing. Thus, a measurement of vibrational frequencies of confined phonons for a variety of diffusion annealed isotope superlattices allows us to precisely determine the Si self-diffusivity $D_{\text{Si}}^{\text{SD}}(T)$ for a given temperature.

Figure 1 shows Raman spectra of the $^{28}\text{Si}_{20}/^{30}\text{Si}_{20}$ isotope superlattice annealed at 815°C for various durations t . Raman peaks of the confined LO phonons observed clearly on the left side of the large LO peak of $^{\text{nat}}\text{Si}$ in the as-grown sample correspond to $\text{LO}_3(^{28}\text{Si})$, $\text{LO}_5(^{28}\text{Si})$, and $\text{LO}_1(^{30}\text{Si})$ in the order from the higher to lower Raman shifts, respectively. Here the notations $\text{LO}_m(^{28}\text{Si})$ and $\text{LO}_m(^{30}\text{Si})$ represent the m th confined vibrational mode in the ^{28}Si and ^{30}Si layers, respectively, as was introduced originally for confined phonons in Ge isotope superlattices [25]. Interdiffusion of isotopes at every $^{28}\text{Si}/^{30}\text{Si}$ interface in the superlattices occurs exactly in the same manner. Therefore, peak positions of the confined phonons shift systematically with the diffusion annealing time t . For example, as t increases, the lowest Raman shift peak $\text{LO}_1(^{30}\text{Si})$ disappears, while the $\text{LO}_1(^{28}\text{Si})$ hidden in the $^{\text{nat}}\text{Si}$ substrate peak emerges after 12 h annealing. $D_{\text{Si}}^{\text{SD}}(T)$ for a given temperature is obtained by quantitative comparison with a theoretical calculation using the planar bond-charge model [26], which allows us to calculate precisely the frequencies of confined phonons in a given Si isotope superlattice as we have demonstrated in Ref. [13].

Figure 2 shows direct comparison of the frequencies of the confined LO phonons between the experiment and

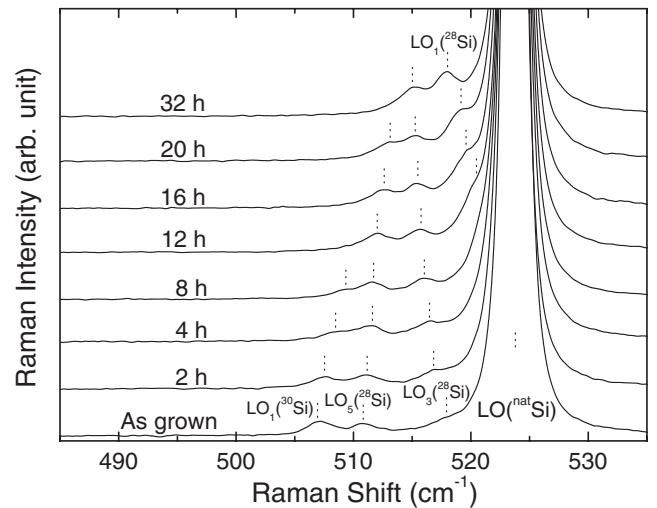


FIG. 1. Raman spectra of the $^{28}\text{Si}_{20}/^{30}\text{Si}_{20}$ isotope superlattice annealed at 815°C for various durations as labeled in the figure.

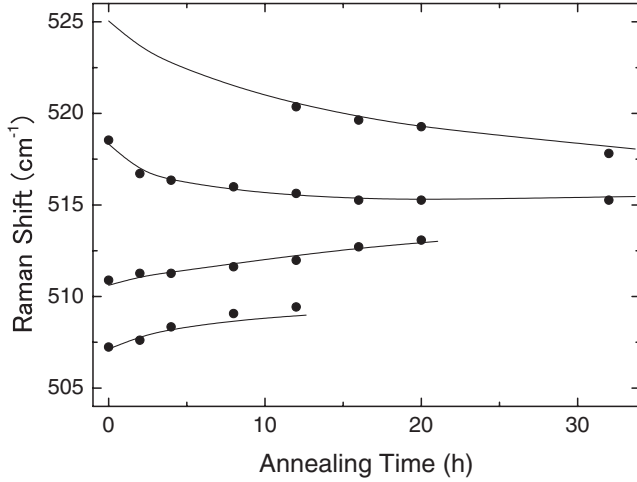


FIG. 2. Annealing time dependence of the Raman shifts of the localized phonons in the $^{28}\text{Si}_{20}/^{30}\text{Si}_{20}$ isotope superlattice. The annealing temperature was 815°C . Solid circles are experimental LO phonon frequencies determined from the peak positions in Fig. 1. Solid lines are a theoretical calculation of the confined peak frequencies using $D_{\text{Si}}^{\text{SD}} = 6.4 \times 10^{-20} \text{ cm}^2/\text{s}$.

calculation for the 815°C annealed samples shown in Fig. 1. Solid circles are the experimentally determined peak positions, while solid curves are the calculation by the planar bond-charge model using $D_{\text{Si}}^{\text{SD}}(815^\circ\text{C}) = 6.4 \times 10^{-20} \text{ cm}^2/\text{s}$. Note that $D_{\text{Si}}^{\text{SD}}(T)$ is the only adjustable parameter in the model, and the excellent agreement between the experiment and calculation as shown in Fig. 2 is achieved only with a single $D_{\text{Si}}^{\text{SD}}(T)$ with the tolerance much less than a few percent. Figure 3 shows the annealing time (t) evolution of the depth profile of the ^{30}Si atomic fraction, $C'_{^{30}\text{Si}}$ in the $^{28}\text{Si}_{20}/^{30}\text{Si}_{20}$ isotope superlattice using the Si self-diffusivity $D_{\text{Si}}^{\text{SD}}(815^\circ\text{C}) = 6.4 \times 10^{-20} \text{ cm}^2/\text{s}$ determined for 815°C . The sample prior to

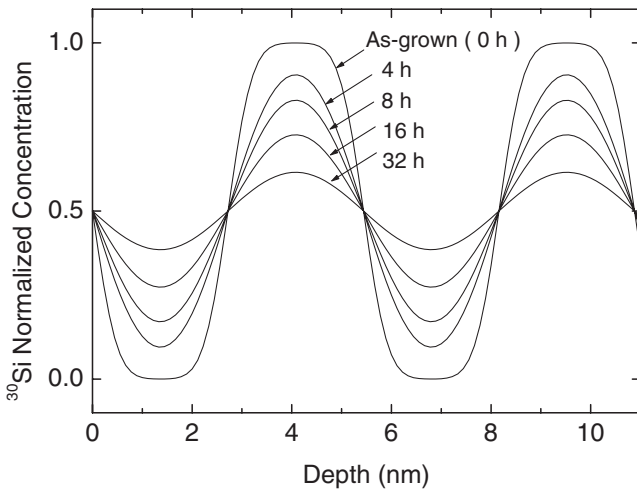


FIG. 3. Calculated annealing time evolution of the depth profile of the ^{30}Si atomic fraction in the $^{28}\text{Si}_{20}/^{30}\text{Si}_{20}$ isotope superlattices for $T = 815^\circ\text{C}$. Experimentally determined $D_{\text{Si}}^{\text{SD}} = 6.4 \times 10^{-20} \text{ cm}^2/\text{s}$ for $T = 815^\circ\text{C}$ is used for this calculation.

annealing has a small interdiffusion characterized by $l \approx 2$. Then the same interdiffusion of ^{28}Si and ^{30}Si isotopes at every $^{28}\text{Si}/^{30}\text{Si}$ interface takes place as the annealing duration increases. Eventually, ^{28}Si and ^{30}Si will be mixed completely for infinitely long annealing, for which the periodicity d_e and d_d disappear, and the phonon modes are characterized as those of the bulk sample having the average mass approximately of ^{29}Si .

Finally, in Fig. 4, the temperature dependence of $D_{\text{Si}}^{\text{SD}}$ determined in the present study is shown by solid circles together with those determined previously by SIMS of isotope heterostructures in open circles [9]. The experimental error of our $D_{\text{Si}}^{\text{SD}}$ is the order of the solid circles representing the data. We stress first that the self-diffusivities determined by the present method agree very well with open circles determined by Bracht *et al.* in the overlapping temperature range between 850 and 900°C . Precise determination of the self-diffusivity by the present method becomes difficult above 900°C , because the periodicities d_e and d_d of the superlattices disappear very quickly (within a few minutes of annealing) due to the large diffusivity at the high temperatures. Therefore, we analyze the solid circles and open circles together to obtain the overall self-diffusivity of Si for $T = 735\text{--}1388^\circ\text{C}$. The solid curve in Fig. 4 is the result of such analysis, and it is expressed by the following equation composed of a sum of two exponential terms:

$$D_{\text{Si}}^{\text{SD}} = 2175.4 \exp\left(\frac{-4.95 \text{ eV}}{k_B T}\right) + 0.0023 \exp\left(\frac{-3.6 \text{ eV}}{k_B T}\right) \text{ cm}^2 \text{ s}^{-1}. \quad (5)$$

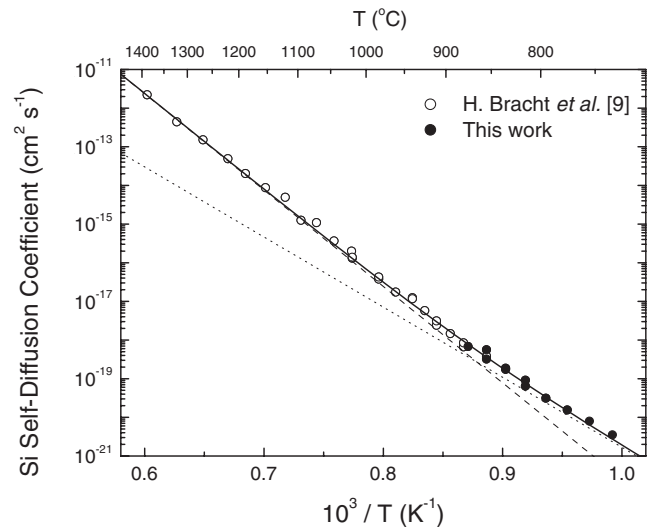


FIG. 4. Temperature dependence of the Si self-diffusivity. Results of the present study are shown by solid circles together with those determined previously by SIMS of isotope heterostructures in open circles [9]. The solid line is the fit described by Eq. (5). Contributions of the self-interstitial and vacancy mechanism are shown by the dashed and dotted lines, respectively. See text for details.

Here the first term represents the self-diffusion due to the self-interstitial mechanism I , and, therefore, the established value of the enthalpy $H_I = 4.95$ eV and prefactor 2175.4 cm² s⁻¹ are assumed from the first place [10]. The remaining two parameters, the enthalpy and prefactor in the second term, were obtained by fitting. The enthalpy $3.6_{-0.1}^{+0.3}$ eV in the second term agrees within the experimental error with the value $H_V = 3.9$ eV determined previously for Si self-diffusion in vacancy-rich Si single crystals [23]. Thus, it is reasonable to conclude that the experimental results in Fig. 4 are the first observation of the crossover from the self-interstitial mechanism at the high temperatures to the vacancy mechanism at the low temperatures. To find the crossover temperature, we separately plot in Fig. 4 the first and second terms in Eq. (5) by dashed and dotted lines, respectively. Their intersect situates approximately at 900 °C. Seeger and Chik have obtained the same 900 °C intersect through very indirect experiments; Ni precipitation assuming Si vacancies are playing the dominant role [27]. Further indirect experiments, in fact, moved this crossover temperature up to 1000 °C and above [14]. The present experiment is the first direct measurement that firmly establishes the crossover temperature of 900 °C.

The enthalpy for the vacancy mechanism H_V is composed of $H_V = H_V^f + H_V^m$, where H_V^f and H_V^m are the formation and migration enthalpies of Si vacancies, respectively. The present $H_V = 3.6_{-0.1}^{+0.3}$ eV together with the most reliable calculation $H_V^f = 3.1$ – 3.6 eV lead to $H_V^m < 0.8$ eV with the most probable value around $H_V^m = 0.4$ eV, which agrees with 0.45 eV obtained with an electron paramagnetic resonance by Watkins [24]. However, the analysis with the most direct experimental $H_V^f = 2.8 \pm 0.3$ eV [21] yields 0.4 eV $< H_V^m < 1.4$ eV with the most probable value around 0.8 eV. Thus, while further experiments are needed, our analysis indicates that H_V^m is likely to be less than 1 eV even at the annealing temperatures employed in this study.

In summary, the crossover between the self-interstitial and vacancy mechanisms were experimentally observed for the first time at 900 °C, and, therefore, $H_V = H_V^f + H_V^m = 3.6$ eV is established firmly. This finding is of great technological importance since the process simulation of state-of-the-art Si electronic devices requires precise values of Si self-diffusivity. The present study has shown that the self-diffusivity at $T < 900$ °C is much larger than what has been employed as a standard [9].

We acknowledge Dr. H. Bracht (Münster University) for fruitful discussion and T. Mouri and A. Fujimoto (Keio University) for technical support. This work has been supported in part by the Research Program on Collaborative Development of Innovative Seeds by JST.

*Electronic address: kitoh@appi.keio.ac.jp

- [1] H. Seong and L.J. Lewis, Phys. Rev. B **53**, 9791 (1996).
- [2] M.J. Puska, S. Pöykkö, M. Pesola, and R.M. Nieminen, Phys. Rev. B **58**, 1318 (1998).
- [3] A. Antonelli, E. Kaxiras, and D.J. Chadi, Phys. Rev. Lett. **81**, 2088 (1998).
- [4] M.I.J. Probert and M.C. Payne, Phys. Rev. B **67**, 075204 (2003).
- [5] J. Lento and R.M. Nieminen, J. Phys. Condens. Matter **15**, 4387 (2003).
- [6] F. El-Mellouhi, N. Mousseau, and P. Ordejón, Phys. Rev. B **70**, 205202 (2004).
- [7] Y. Kumeda, D.J. Wales, and L.J. Munro, Chem. Phys. Lett. **341**, 185 (2001).
- [8] D. Caliste and P. Pochet, Phys. Rev. Lett. **97**, 135901 (2006).
- [9] H. Bracht, E.E. Haller, and R. Clark-Phelps, Phys. Rev. Lett. **81**, 393 (1998).
- [10] H. Bracht, N.A. Stolwijk, and H. Mehrer, Phys. Rev. B **52**, 16542 (1995).
- [11] E. Silveira, W. Dondl, G. Abstreiter, and E.E. Haller, Phys. Rev. B **56**, 2062 (1997).
- [12] T. Kojima, R. Nebashi, K.M. Itoh, and Y. Shiraki, Appl. Phys. Lett. **83**, 2318 (2003).
- [13] Y. Shimizu and K.M. Itoh, Thin Solid Films **508**, 160 (2006).
- [14] T.Y. Tan and U. Gösele, Appl. Phys. A **37**, 1 (1985).
- [15] P.M. Fahey, P.B. Griffin, and J.D. Plummer, Rev. Mod. Phys. **61**, 289 (1989).
- [16] A. Ural, P.B. Griffin, and J.D. Plummer, Phys. Rev. Lett. **83**, 3454 (1999).
- [17] H. Bracht, Physica (Amsterdam) **376B–377B**, 11 (2006).
- [18] A. Giese, H. Bracht, N.A. Stolwijk, and D. Baither, Mater. Sci. Eng. B **71**, 160 (2000).
- [19] K. Compaan and Y. Haven, Trans. Faraday Soc. **54**, 1498 (1958).
- [20] K. Compaan and Y. Haven, Trans. Faraday Soc. **52**, 786 (1956).
- [21] V. Ranki and K. Saarinen, Phys. Rev. Lett. **93**, 255502 (2004).
- [22] L. Lerner and N.A. Stolwijk, Appl. Phys. Lett. **86**, 011901 (2005).
- [23] H. Bracht, J.F. Pedersen, N. Zangenberg, A.N. Larsen, E.E. Haller, G. Lulli, and M. Posselt, Phys. Rev. Lett. **91**, 245502 (2003).
- [24] G.D. Watkins, Mater. Res. Soc. Symp. Proc. **469**, 139 (1997).
- [25] J. Spitzer, T. Ruf, M. Cardona, W. Dondl, R. Schorer, G. Abstreiter, and E.E. Haller, Phys. Rev. Lett. **72**, 1565 (1994).
- [26] P. Molinàs-Mata and M. Cardona, Phys. Rev. B **43**, 9799 (1991); P. Molinàs-Mata, A.J. Shields, and M. Cardona, *ibid.* **47**, 1866 (1993).
- [27] A. Seeger and K.P. Chik, Phys. Status Solidi **29**, 455 (1968).